Inorganic Chemistry
Article

Inorg. Chem. **2010**, *49*, 1595–1606 **1595**
DOI: 10.1021/ic901986w

Experimental Evidence for Magnetic Exchange in Di- and Trinuclear Uranium(IV) Ethynylbenzene Complexes

Brian S. Newell, Anthony K. Rappé, and Matthew P. Shores*

Department of Chemistry, Colorado State University, Fort Collins, Colorado 80523−1872

Received October 8, 2009

We report the preparation and magnetic property investigations of a structurally related family of mono-, di-, and trinuclear U(IV) aryl acetylide complexes. The reaction between $[(NN'_3)UCl]$ and lithiated aryl acetylides leads to the formation of the hexacoordinate complexes $[(NN'_3)U(CCPh)_2(Li\cdot THF)]$ (**1**) and $[(NN'_3)_2U_2(p\text{-DEB})(THF)]$ (**2**) as red-brown and yellow-green crystalline solids, respectively. In contrast, combining the uranacycle $[(bit\text{-}NN'_3)U]$ (bit-NN'_3 = $[N(CH_2CH_2NSi^tBuMe_2)_2(CH_2CH_2Si^tBuMeCH_2])$ with stoichiometric amounts of mono-, bis-, and tris(ethynyl) benzenes affords the yellow-green pentacoordinate arylacetylide complexes $[(NN'_3)U(CCPh)]$ (**3**), $[(NN'_3)_2U_2(m\text{-DEB})]$ (**4**), $[(NN'_3)_2U_2(p\text{-DEB})]$ (**5**), and $[(NN'_3)_3U_3(TEB)]$ (**6**), where NN'_3 = $[N(CH_2CH_2NSi^tBuMe_2)_3]$. The measured magnetic susceptibilities for **1**−**6** trend toward non-magnetic ground states at low temperatures. Nevertheless, the di- and trinuclear pentacoordinate compounds **4**−**6** appear to display weak magnetic communication between the uranium centers. This communication is modeled by fitting of the direct current (DC) magnetic susceptibility data, using the spin Hamiltonian $\hat{H} = -2J(\hat{S}_i\cdot\hat{S}_j)$. These results are consistent with weak ferromagnetic coupling for complexes 4−**6** (J = 4.76, 2.75, and 1.11 cm^{-1}, respectively), while the fit for **2** is consistent with a near-negligible exchange interaction (J = −0.05 cm^{-1}). Geometry-optimized Stuttgart/6-31 g* B3LYP hybrid DFT calculations were carried out (spin−orbit coupling omitted) on model complexes of **3**−**5**. The mononuclear complex shows a triplet ground state with singly occupied degenerate f orbitals. The meta- and para-bridged species are computed to show very weak ferro- and antiferromagnetic coupling, respectively. All three complexes show only small net spin density on the acetylide-containing ligands. The monomeric phenylacetylide complex **3** undergoes a reversible redox couple at −1.02 V versus $[Cp_2Fe]^{+/0}$, assignable to an oxidation of U(IV) to U(V).

Introduction

The electronic structures of actinide-containing complexes feature a rich interplay of orbital interactions, spin−orbit coupling, and electron correlation, whose understanding is critical to using actinides in fuels or catalysis, and to settle longstanding questions about the role of f orbitals in metal−ligand bonding.[1−10] The magnetic properties of actinide complexes represent a mixing of characteristics normally associated with transition metal ions (e.g., superexchange) and lanthanides (e.g., spin−orbit coupling),[11] and can be used to probe electronic structure in detail. Thus, combining magnetochemical studies with high level calculations offers a pathway for understanding this unique group of compounds.

In addition to fundamental interest in electronic structure, recent work in f-element magnetochemistry is motivated by the potential for these species to contribute to the development of single-molecule magnets (SMMs).[12−15] These monodisperse superparamagnetic particles exhibit a thermal barrier to magnetic spin reorientation, and may eventually

*To whom correspondence should be addressed. E-mail: shores@lamar.colostate.edu.

(1) Andrea, T.; Eisen, M. S. *Chem. Soc. Rev.* **2008**, *37*, 550–567.
(2) Ephritikhine, M. *Dalton Trans.* **2006**, 2501–2516.
(3) Fox, A. R.; Bart, S. C.; Meyer, K.; Cummins, C. C. *Nature* **2008**, *455*, 341–349.
(4) Schnaars, D. D.; Wu, G.; Hayton, T. W. *Dalton Trans.* **2008**, 6121–6126.
(5) Denning, R. G. *J. Phys. Chem. A* **2007**, *111*, 4125–4143.
(6) Gaunt, A. J.; Reilly, S. D.; Enriquez, A. E.; Scott, B. L.; Ibers, J. A.; Sekar, P.; Ingram, K. I. M.; Kaltsoyannis, N.; Neu, M. P. *Inorg. Chem.* **2008**, *47*, 29–41.
(7) Jensen, M. P.; Bond, A. H. *J. Am. Chem. Soc.* **2002**, *124*, 9870–9877.
(8) Choppin, G. R. *J. Alloys Compd.* **2002**, *344*, 55–59.
(9) Mazzanti, M.; Wietzke, R. L.; Pecaut, J.; Latour, J. M.; Maldivi, P.; Remy, M. *Inorg. Chem.* **2002**, *41*, 2389–2399.
(10) Miguirditchian, M.; Guillaneux, D.; Guillaumont, D.; Moisy, P.; Madic, C.; Jensen, M. P.; Nash, K. L. *Inorg. Chem.* **2005**, *44*, 1404–1412.
(11) Rinehart, J. D.; Harris, T. D.; Kozimor, S. A.; Bartlett, B. M.; Long, J. R. *Inorg. Chem.* **2009**, *48*, 3382–3395.
(12) Sessoli, R.; Tsai, H. L.; Schake, A. R.; Wang, S. Y.; Vincent, J. B.; Folting, K.; Gatteschi, D.; Christou, G.; Hendrickson, D. N. *J. Am. Chem. Soc.* **1993**, *115*, 1804–1816.
(13) Sessoli, R.; Gatteschi, D.; Caneschi, A.; Novak, M. A. *Nature* **1993**, *365*, 141–143.
(14) Aromi, G.; Brechin, E. K. In *Single-Molecule Magnets and Related Phenomena*; Winpenny, R., Ed.; Springer: Berlin, **2006**; Vol. *122*, pp 1−67.
(15) Milios, C. J.; Inglis, R.; Vinslava, A.; Bagai, R.; Wernsdorfer, W.; Parsons, S.; Perlepes, S. P.; Christou, G.; Brechin, E. K. *J. Am. Chem. Soc.* **2007**, *129*, 12505–12511.

Published on Web 01/19/2010

find use in data storage,[16,17] quantum computing,[18−23] or refrigeration applications.[24,25] However, their exploitation awaits variants that can display magnetic bistability at more practical temperatures than the ∼4.5 K currently observed.[15] Here, incorporation of paramagnetic lanthanide ions have received attention, since spin−orbit coupling and relativistic effects common to those ions can engender the large single-ion anisotropies necessary for slow magnetization relaxation behavior.[26−36] Several complexes have properties consistent with SMMs, such as the observation of frequency-dependent out-of-phase alternating current (AC) susceptibility signals.[37−42] A drawback to the approach is that the "buried" 4f orbitals in lanthanides participate only weakly in bonding interactions, leading to marginal exchange coupling with neighboring spin centers;[43−45] this ultimately limits the maximum temperature at which the magnetic bistability occurs.

Alternatively, all of the above-mentioned attributes can be found in the early actinides, with the added benefit of larger, more diffuse 5f orbitals capable of stronger bonding and exchange interactions.[46−51] However, the dynamic magnetic properties of actinide complexes are less well-known, in part because of difficulties in determining ligand field parameters and the complications arising from relativistic effects as well as d and f electron correlations.[38,52] Nevertheless, recent reports indicate that synthetic efforts toward paramagnetic actinide-containing assemblies offer diverse and interesting magnetism. A Th_6Mn_{10} cluster shows that even f^0 species may contribute to the observation of frequency-dependent out-of-phase susceptibility signals.[26] Coupling between uranium and transition metal ions has been investigated, and ferromagnetic communication between transition metal ions and cubic U(IV) centers has been demonstrated in molecular species.[11,47−50,53−56] Also relevant to the work to be presented here, Anderson's dinuclear complex $[((MeC_5H_4)_3U)_2(\mu\text{-}1,4\text{-}N_2C_6H_4)]$ illustrates the viability of U(V)−U(V) magnetic exchange via f orbitals.[57] Further advancement in this area hinges on improving synthetic control over paramagnetic uranium ligand field and spin−orbit parameters, so as to optimize exchange coupling between uranium and transition-metal species, and ultimately to control molecular magnetic anisotropy.

The purpose of the present study is to investigate coordination geometry effects on U(IV) magnetic properties. It is well-known that the $5f^2$ electronic configuration gives diamagnetic ground states when the U(IV) coordination geometry is octahedral, but exhibits paramagnetic ground states ($S = 1$) when the U(IV) ion is surrounded by a cubic ligand field.[48−50,52−56,58,59] We wondered if a trigonal bipyramidal (tbp) coordination geometry may offer another way for U(IV) to show paramagnetic ground states. In this case, group theory predicts a doubly degenerate e'' ground state, which should result in an $S = 1$ species.[58] We note that

(16) Long, J. R. *Chemistry of Nanostructured Materials*; World Scientific: Hong Kong, 2003.
(17) Bogani, L.; Wernsdorfer, W. *Nat. Mater.* **2008**, *7*, 179–186.
(18) Friedman, J. R.; Sarachik, M. P.; Tejada, J.; Ziolo, R. *Phys. Rev. Lett.* **1996**, *76*, 3830–3833.
(19) Thomas, L.; Lionti, F.; Ballou, R.; Gatteschi, D.; Sessoli, R.; Barbara, B. *Nature* **1996**, *383*, 145–147.
(20) Gatteschi, D.; Sessoli, R. *Angew. Chem., Int. Ed.* **2003**, *42*, 268–297.
(21) Wernsdorfer, W.; Sessoli, R. *Science* **1999**, *284*, 133–135.
(22) Leuenberger, M. N.; Loss, D. *Nature* **2001**, *410*, 789–793.
(23) Affronte, M.; Troiani, F.; Ghirri, A.; Carretta, S.; Santini, P.; Corradini, V.; Schuecker, R.; Muryn, C.; Timco, G.; Winpenny, R. E. *Dalton Trans.* **2006**, 2810–2817.
(24) Ciasca, G.; De Seta, M.; Capellini, G.; Evangelisti, F.; Ortolani, M.; Virgilio, M.; Grosso, G.; Nucara, A.; Calvani, P. *Phys. Rev. B* **2009**, *79*, 7.
(25) Evangelisti, M.; Candini, A.; Ghirri, A.; Affronte, M.; Brechin, E. K.; McInnes, E. J. L. *Appl. Phys. Lett.* **2005**, *87*, 3.
(26) Mishra, A.; Tasiopoulos, A. J.; Wernsdorfer, W.; Abboud, K. A.; Christou, G. *Inorg. Chem.* **2007**, *46*, 3105–3115.
(27) Costes, J. P.; Auchel, M.; Dahan, F.; Peyrou, V.; Shova, S.; Wernsdorfer, W. *Inorg. Chem.* **2006**, *45*, 1924–1934.
(28) Hamamatsu, T.; Yabe, K.; Towatari, M.; Osa, S.; Matsumoto, N.; Re, N.; Pochaba, A.; Mrozinski, J.; Gallani, J. L.; Barla, A.; Imperia, P.; Paulsen, C.; Kappler, J. P. *Inorg. Chem.* **2007**, *46*, 4458–4468.
(29) Mishra, A.; Wernsdorfer, W.; Abboud, K. A.; Christou, G. *J. Am. Chem. Soc.* **2004**, *126*, 15648–15649.
(30) Zaleski, C. M.; Depperman, E. C.; Kampf, J. W.; Kirk, M. L.; Pecoraro, V. L. *Angew. Chem., Int. Ed.* **2004**, *43*, 3912–3914.
(31) Gao, S.; Su, G.; Yi, T.; Ma, B. Q. *Phys. Rev. B* **2001**, *63*, 054431.
(32) Mereacre, V. M.; Ako, A. M.; Clerac, R.; Wernsdorfer, W.; Filoti, G.; Bartolome, J.; Anson, C. E.; Powell, A. K. *J. Am. Chem. Soc.* **2007**, *129*, 9248–9249.
(33) Papatriantafyllopoulou, C.; Estrader, M.; Efthymiou, C. G.; Dermitzaki, D.; Gkotsis, K.; Terzis, A.; Diaz, C.; Perlepes, S. P. *Polyhedron* **2009**, *28*, 1652–1655.
(34) Klokishner, S. I.; Ostrovsky, S. M.; Reu, O. S.; Palii, A. V.; Tregenna-Piggott, P. L. W.; Brock-Nannestad, T.; Bendix, J.; Mutka, H. *J. Phys. Chem. C* **2009**, *113*, 8573–8582.
(35) Mereacre, V.; Prodius, D.; Ako, A. M.; Kaur, N.; Lipkowski, J.; Simmons, C.; Dalal, N.; Geru, I.; Anson, C. E.; Powell, A. K.; Turta, C. *Polyhedron* **2008**, *27*, 2459–2463.
(36) Sorace, L.; Sangregorio, C.; Figuerola, A.; Benelli, C.; Gatteschi, D. *Chem.—Eur. J.* **2009**, *15*, 1377–1388.
(37) Ishikawa, N.; Sugita, M.; Ishikawa, T.; Koshihara, S.; Kaizu, Y. *J. Am. Chem. Soc.* **2003**, *125*, 8694–8695.
(38) Ishikawa, N.; Sugita, M.; Ishikawa, T.; Koshihara, S.; Kaizu, Y. *J. Phys. Chem. B* **2004**, *108*, 11265–11271.
(39) Ishikawa, N.; Sugita, M.; Wernsdorfer, W. *J. Am. Chem. Soc.* **2005**, *127*, 3650–3651.
(40) Ishikawa, N.; Sugita, M.; Wernsdorfer, W. *Angew. Chem., Int. Ed.* **2005**, *44*, 2931–2935.
(41) AlDamen, M. A.; Clemente-Juan, J. M.; Coronado, E.; Martí-Gastaldo, C.; Gaita-Ariño, A. *J. Am. Chem. Soc.* **2008**, *130*, 8874–8875.
(42) Gamer, M. T.; Lan, Y.; Roesky, P. W.; Powell, A. K.; Clérac, R. *Inorg. Chem.* **2008**, *47*, 6518–6583.
(43) Kahn, M. L.; Mathoniere, C.; Kahn, O. *Inorg. Chem.* **1999**, *38*, 3692–3697.
(44) Benelli, C.; Gatteschi, D. *Chem. Rev.* **2002**, *102*, 2369–2387.
(45) Costes, J. P.; Dahan, F.; Dupuis, A.; Laurent, J. P. *Chem.—Eur. J.* **1998**, *4*, 1616–1620.
(46) Kaltsoyannis, N.; Scott, P. *The f Elements*; Oxford University Press: New York, 1999.
(47) Monreal, M. J.; Diaconescu, P. L. *Organometallics* **2008**, *27*, 1702–1706.
(48) Diaconescu, P. L.; Arnold, P. L.; Baker, T. A.; Mindiola, D. J.; Cummins, C. C. *J. Am. Chem. Soc.* **2000**, *122*, 6108–6109.
(49) Kozimor, S. A.; Bartlett, B. M.; Rinehart, J. D.; Long, J. R. *J. Am. Chem. Soc.* **2007**, *129*, 10672–10674.
(50) Rinehart, J. D.; Bartlett, B. M.; Kozimor, S. A.; Long, J. R. *Inorg. Chem. Acta* **2008**, *361*, 3534–3538.
(51) Gaunt, A. J.; Reilly, S. D.; Enriquez, A. E.; Scott, B. L.; Ibers, J. A.; Sekar, P.; Ingram, K. I. M.; Kaltsoyannis, N.; Neu, M. P. *Inorg. Chem.* **2008**, *47*, 29–41.
(52) Schelter, E. J.; Veauthier, J. M.; Thompson, J. D.; Scott, B. L.; John, K. D.; Morris, D. E.; Kiplinger, J. L. *J. Am. Chem. Soc.* **2006**, *128*, 2198–2199.
(53) Salmon, L.; Thuery, P.; Riviere, E.; Ephritikhine, M. *Inorg. Chem.* **2006**, *45*, 83–93.
(54) Graves, C. R.; Yang, P.; Kozimor, S. A.; Vaughn, A. E.; Clark, D. L.; Conradson, S. D.; Schelter, E. J.; Scott, B. L.; Thompson, J. D.; Hay, P. J.; Morris, D. E.; Kiplinger, J. L. *J. Am. Chem. Soc.* **2008**, *130*, 5272–5285.
(55) Schelter, E. J.; Wu, R. L.; Scott, B. L.; Thompson, J. D.; Morris, D. E.; Kiplinger, J. L. *Angew. Chem., Int. Ed.* **2008**, *47*, 2993–2996.
(56) Kiplinger, J. L.; Scott, B. L.; Schelter, E. J.; Tournear, J. *J. Alloys Compd.* **2007**, *444*, 477–482.
(57) Rosen, R. K.; Andersen, R. A.; Edelstein, N. M. *J. Am. Chem. Soc.* **1990**, *112*, 4588–4590.
(58) Figgis, B. N.; Hitchman, M. A. *Ligand Field Theory and Its Applications*; Wiley-VCH: New York, 2000.
(59) Edwards, P. G.; Andersen, R. A.; Zalkin, A. *J. Am. Chem. Soc.* **1981**, *103*, 7792–7794.

predicting the level of splitting of the f orbitals because of ligand field effects alone is complicated by the substantial spin−orbit coupling present in the actinides.[60] It is also known that many low symmetry U(IV) complexes give "non-magnetic" ground states.[61] Nevertheless, monomeric tbp U(IV) phenylacetylide complexes in which triamidoamine (NN'_3) ligands occupy the other coordination sites offer synthetic precedent for enforcing 5-coordinate geometries,[62−66] and to our knowledge the magnetic properties of these species have not been studied in detail. In addition, ethynylbenzene ligands have been demonstrated to be efficient communicators of spin information between paramagnetic transition metal species.[67,68] Thus, the combination of [(NN'_3)U] species with bridging aryl acetylide ligands may be expected to give rise to di- and trinuclear assemblies by which uranium magnetochemistry may be tuned structurally.

Herein, we describe the preparation and (magneto)structural characterization of di- and trinuclear penta- and hexacoordinate U(IV) species bridged by aryl acetylides. The experimental and theoretical assessment of exchange coupling in these species provides evidence for weak exchange coupling operative between pentacoordinate U(IV) centers.

Experimental Section

Preparation of Compounds. All manipulations were carried out either inside a dinitrogen-filled glovebox (MBRAUN Labmaster 130) or via standard Schlenk techniques on a N_2 manifold. Pentane was distilled over sodium metal, degassed (freeze−pump−thawed 3 × 20 min) and stored under an atmosphere of dinitrogen. All other solvents were reagent grade, passed through alumina, degassed, and stored under dinitrogen. The compounds UCl_4,[69] [$Li_3(NN'_3)(THF)_3$] (where NN'_3 = [$N(CH_2CH_2NSi^tBuMe_2)_3$]),[70] [(NN'_3)UCl],[71] [(*bit*-NN'_3)U] (where *bit*-NN'_3 = [$N(CH_2CH_2NSi^tBuMe_2)(CH_2CH_2Si^tBuMeCH_2]$),[63] [($NN'_3$)U(CCPh)] (**3**),[63] and 1,3,5-triethynylbenzene[72] (H_3TEB) were prepared according to the literature, except that sublimation was not carried out on the [(NN'_3)UCl] complex. The acetylene ligands 1,4- and 1,3-diethynylbenzene (*p*-H_2DEB and *m*-H_2DEB, respectively) were purchased from Sigma and were sublimed or distilled, respectively, before use. The lithiated acetylides, lithium phenylacetylide and Li_2(*p*-DEB), were synthesized by reacting the appropriate stoichiometric amount of *n*-BuLi with the corresponding free acetylene in pentane. The solids were collected, dried in vacuo, and used without further characterization. All other reagents were obtained from commercial vendors and used without further purification.

Caution! *Depleted uranium (primary isotope ^{238}U) is a weak α emitter (4.197 MeV) with a half-life of 4.47×10^9 years; manipulations and reactions should be carried out in monitored fume hoods or in an inert atmosphere glovebox in a radiation laboratory equipped with α- and β-counting equipment.*

[(NN'_3)U(CCPh)$_2$(Li·THF)] (1). Solid, recrystallized [(NN'_3)UCl] (0.198 g, 0.261 mmol) was combined with lithium phenylacetylide (0.057 g, 0.53 mmol) and 15 mL of pentane. The yellow-green mixture was stirred at room temperature for 1 h. Subsequent addition of 2 mL of tetrahydrofuran (THF) resulted in a color change to red-brown. The mixture was stirred at room temperature for 1 h, and then filtered to remove LiCl. Volatiles were removed from the filtrate in vacuo to afford a red-brown residue. This was extracted into 10 mL of pentane, concentrated to about 5 mL under reduced pressure, and left at ambient temperature for 8 h, at which point several red-brown crystals were observed. The product was collected by filtration, dried in vacuo, and recrystallized from hot pentane to afford a deep red crystalline solid (0.121 g, 46% yield based on [(NN'_3)UCl]). Single crystals suitable for X-ray analysis were grown from a concentrated pentane solution maintained at −34 °C for 8 h. Absorption spectrum (pentane) λ_{max} (ε_M): 686 nm (95 L·mol^{-1}·cm^{-1}). ^{1}H NMR (293 K, C_6D_6): δ 8.09 (br, 6H, CH_2), 7.39 (d, 4H, THF), 7.06 (br, 4H, aryl), 6.90 (m, 6H, aryl), 5.22 (s, 27H, ^{t}Bu), 4.01 (s, 18H, Me_2Si), 1.50 (d, 4H, THF), −16.39 ppm (br, 6H, CH_2). IR (mineral oil): $\nu_{C\equiv C}$ 2044 cm^{-1}. Magnetic susceptibility (SQUID, 300 K): μ_{eff} = 2.14 μ_B. Anal. Calcd for $C_{44}H_{75}N_4OSi_3ULi$: C, 52.57; H, 7.52; N, 5.57. Found: C, 52.38; H, 7.76; N, 5.52.

[(NN'_3)$_2$U$_2$(*p*-DEB)(THF)] (2). Solid [(NN'_3)UCl] (0.500 g, 0.659 mmol) was combined with Li_2(*p*-DEB) (0.045 g, 0.330 mmol) and 5 mL of toluene. The resulting brown-green mixture was stirred at ambient temperature for 8 h, filtered to remove LiCl, concentrated to about 2 mL under reduced pressure, and then cooled to −34 °C. After 8 h, a yellow-green crystalline precipitate was observed. The crude product was collected by filtration, dried in vacuo, and recrystallized from hot pentane to afford a yellow crystalline solid (0.152 g, 28% yield based on [(NN'_3)UCl]). Single crystals of [(NN'_3)$_2$U$_2$(*p*-DEB)(THF)$_2$]·C_5H_{12} (**2**·THF·C_5H_{12}) suitable for X-ray analysis were grown from a concentrated pentane solution maintained at −34 °C for 8 h. Absorption spectrum (pentane) λ_{max} (ε_M): 501 (406), 528 (326), 587 (212), 606 (176), 687 nm (320 L·mol^{-1}·cm^{-1}). IR (mineral oil): $\nu_{C\equiv C}$ 2061 cm^{-1}. Magnetic susceptibility (SQUID, 300 K): μ_{eff} = 4.73 μ_B. Anal. Calcd for $C_{62}H_{126}N_8OSi_6U_2$: C, 45.29; H, 7.72; N, 6.81. Found: C, 45.07; H, 7.22; N, 6.81.

[(NN'_3)U(CCPh)] (3). A solution of phenylacetylene in 1 mL of pentane (80 μL, 0.73 mmol) was added dropwise to a stirred solution of [(*bit*-NN'_3)U] (0.539 g, 0.745 mmol) in 10 mL of pentane at −78 °C, and the resulting yellow-green solution was warmed to room temperature and stirred for 3 h. The solution was filtered, concentrated to about 2 mL under reduced pressure, and then cooled to −34 °C. After 8 h, a yellow-green microcrystalline precipitate was observed. The crude product was collected by filtration, dried in vacuo, and recrystallized from hot pentane to afford a yellow-green crystalline solid (0.400 g, 65% based on [(*bit*-NN'_3)U]). Single crystals suitable for X-ray analysis were grown from a concentrated pentane solution maintained at −34 °C for 8 h. Absorption spectrum (pentane) λ_{max} (ε_M): 281 (4800), 485 (42), 503 (44), 529 (48), 587 (26), 614 (19), 621 (19), 629 (18), 650 (16), 654 (16), 658 (17), 687 (75), 691 (70), 719 (20), 803 (12), 828 (13), 880 (12), 924 (12), 961 nm (10 L·mol^{-1}·cm^{-1}). ^{1}H NMR (293 K, C_6D_6): δ 8.09 (s, 6H, CH_2), 5.23 (s, 27H, ^{t}Bu), 4.02 (s, 18H, Me_2Si), 3.37 (m, 2H, aryl), 1.52 (d, 2H, aryl), 1.51 (s, 1H, aryl), −16.35 ppm (s, 6H, CH_2). IR (mineral oil): $\nu_{C\equiv C}$ 2054 cm^{-1}. Magnetic susceptibility

(60) Cotton, S. *Lanthanide and Actinide Chemistry*; Wiley: West Sussex, 2006.
(61) Schelter, E. J.; Yang, P.; Scott, B. L.; Thompson, J. D.; Martin, R. L.; Hay, P. J.; Morris, D. E.; Kiplinger, J. L. *Inorg. Chem.* **2007**, *46*, 7477–7488.
(62) Gebala, A. E.; Tsutsui, M. *J. Am. Chem. Soc.* **1973**, *95*, 91–93.
(63) Boaretto, R.; Roussel, P.; Alcock, N. W.; Kingsley, A. J.; Munslow, I. J.; Sanders, C. J.; Scott, P. *J. Organomet. Chem.* **1999**, *591*, 174–184.
(64) Roussel, P.; Hitchcock, P. B.; Tinker, N.; Scott, P. *Chem. Commun.* **1996**, 2053–2054.
(65) Le Borgne, T.; Riviere, E.; Marrot, J.; Thuery, P.; Girerd, J. J.; Ephritikhine, M. *Chem.—Eur. J.* **2002**, *8*, 774–783.
(66) Roussel, P.; Hitchcock, P. B.; Tinker, N. D.; Scott, P. *Inorg. Chem.* **1997**, *36*, 5716–5721.
(67) Weyland, T.; Costuas, K.; Mari, A.; Halet, J. F.; Lapinte, C. *Organometallics* **1998**, *17*, 5569–5579.
(68) Paul, F.; Bondon, A.; Costa, G.; Malvolti, F.; Sinbandhit, S.; Cador, O.; Costuas, K.; Toupet, L.; Boillot, M-L. *Inorg. Chem.* **2009**, *48*, 10608–10624.
(69) Hermann, J. A.; Suttle, J. F. *Inorg. Synth.* **1957**, *5*, 143–145.
(70) Roussel, P.; Alcock, N. W.; Scott, P. *Inorg. Chem.* **1998**, *37*, 3435–3436.
(71) Roussel, P.; Alcock, N. W.; Boaretto, R.; Kingsley, A. J.; Munslow, I. J.; Sanders, C. J.; Scott, P. *Inorg. Chem.* **1999**, *38*, 3651–3656.
(72) Royles, B. J. L.; Smith, D. M. *J. Chem. Soc., Perkin Trans. 1* **1994**, 355–358.

Table 1. Crystallographic Data[a] for Compounds $[(NN'_3)U(CCPh)_2(Li\cdot THF)]$ (**1**), $[(NN'_3)_2U_2(p\text{-DEB})(THF)_2]\cdot C_5H_{12}$ (**2**·THF·C_5H_{12}), $[(NN'_3)U(CCPh)]$ (**3**), $[(NN'_3)_2U_2(m\text{-DEB})]\cdot C_5H_{12}$ (**4**·C_5H_{12}), and $[(NN'_3)_2U_2(p\text{-DEB})]\cdot C_5H_{12}$ (**5**·C_5H_{12})

	1	**2**·THF·C_5H_{12}	**3**	**4**·C_5H_{12}	**5**·C_5H_{12}
formula	$C_{44}H_{75}N_4OSi_3ULi$	$C_{66}H_{134}N_8O_2Si_6U_2$	$C_{32}H_{62}N_4Si_3U$	$C_{63}H_{130}N_8Si_6U_2$	$C_{63}H_{130}N_8Si_6U_2$
formula wt	1005.32	1788.56	825.16	1644.35	1644.35
color, habit	red/brown needle	yellow/green block	yellow/green rod	yellow/green rod	yellow/green cube
T, K	100(2)	100(2)	100(2)	100(2)	100(2)
space group	$P2_1/c$	$P\bar{1}$	$P\bar{1}$	$P2_1/c$	$P2_12_12$
Z	4	2	4	4	4
a, Å	14.6808(3)	16.6289(5)	12.4841(16)	21.6288(13)	23.2529(10)
b, Å	18.0721(4)	16.8054(4)	17.7695(8)	17.3104(10)	18.4727(8)
c, Å	18.8132(3)	17.4480(4)	18.0989(9)	22.1171(13)	19.1547(8)
α, deg		75.127(2)	89.375(3)		
β, deg	96.3540(10)	78.361(2)	89.013(3)	107.924(4)	
γ, deg		67.296(2)	77.136(3)		
V, Å^3	4960.72(17)	4317.19(19)	3913.5(3)	7878.8(8)	8227.8(6)
d_{calc}, g/cm^3	1.346	1.376	1.401	1.386	1.269
GOF	0.99	1.06	1.01	1.06	1.22
$R_1(wR_2)$[b], %	3.36(6.29)	4.35(10.17)	3.42(9.38)	3.17(6.70)	10.54(25.78)

[a] Obtained with graphite-monochromated Mo Kα (λ = 0.71073 Å) radiation. [b] $R_1 = \sum||F_o| - |F_c||/\sum|F_o|$, $wR_2 = \{\sum[w(F_o^2 - F_c^2)^2]/\sum[w(F_o^2)^2]\}^{1/2}$ for all data.

(SQUID, 300 K): μ_{eff} = 3.12 μ_B. Anal. Calcd for $C_{32}H_{62}N_4Si_3U$: C, 46.58; H, 7.57; N, 6.79. Found: C, 46.50; H, 7.21; N, 6.83.

$[(NN'_3)_2U_2$(*m*-DEB)] (4). A solution of *m*-H_2DEB in 1 mL of pentane (37 μL, 0.28 mmol) was added dropwise to a stirred solution of $[(bit\text{-}NN'_3)U]$ (0.407 g, 0.563 mmol) in 10 mL of pentane at −78 °C, and the resulting yellow-green solution was warmed to room temperature and stirred for 3 h. The solution was filtered, concentrated to about 2 mL under reduced pressure, and then cooled to −34 °C. After 8 h, a yellow-green microcrystalline precipitate was observed. The crude product was collected by filtration, dried in vacuo, and recrystallized from hot pentane to afford a yellow-green crystalline solid (0.336 g, 76% based on *m*-H_2DEB). Single crystals suitable for X-ray analysis were grown from a concentrated pentane solution maintained at −34 °C for 8 h. Absorption spectrum (pentane) λ_{max} (ε_M): 281 (11400), 485 (73), 503 (74), 529 (78), 587 (35), 614 (21), 629 (20), 650 (17), 658 (18), 687 (138), 691 (124), 719 (26), 803 (11), 828 (14), 881 (13), 925 (14), 961 nm (11 L·mol^{-1}·cm^{-1}). ^{1}H NMR (293 K, C_6D_6): δ 7.90 (s, 12H, CH_2), 4.77 (s, 54H, ^{t}Bu), 4.62 (br, 2H, aryl), 3.44 (s, 36H, Me_2Si), −0.52 (t, 1H, aryl), −3.96 (s, 1H, aryl), −16.36 ppm (s, 12H, CH_2). IR (mineral oil): $\nu_{C\equiv C}$ 2053 cm^{-1}. Magnetic susceptibility (SQUID, 300 K): μ_{eff} = 4.49 μ_B. Anal. Calcd for $C_{58}H_{118}N_8Si_6U_2$: C, 44.31; H, 7.57; N, 7.12. Found: C, 44.72; H, 7.65; N, 6.69.

$[(NN'_3)_2U_2$(*p*-DEB)] (5). A solution of *p*-H_2DEB in pentane (0.033 g, 0.26 mmol) was added dropwise to a stirred solution of $[(bit\text{-}NN'_3)U]$ (0.402 g, 0.556 mmol) in 10 mL pentane at −78 °C, resulting in the precipitation of a yellow solid. This mixture was warmed to room temperature and stirred for 3 h. The yellow precipitate was collected by filtration, dried in vacuo, and recrystallized from hot toluene to afford a yellow-green crystalline solid (0.362 g, 89% based on *p*-H_2DEB). Single crystals suitable for X-ray analysis were grown from a concentrated toluene solution maintained at −34 °C for 8 h. Absorption spectrum (toluene) λ_{max} (ε_M): 312 (20700), 329 (15800), 363 (4200), 503 (77), 529 (116), 587 (47), 614 (30), 621 (31), 629 (28), 650 (24), 658 (25), 687 (150), 691 (135), 719 (34), 803 (13), 828 (16), 880 (15), 924 (15), 961 nm (12 L·mol^{-1}·cm^{-1}). ^{1}H NMR (293 K, C_6D_6): δ 8.07 (s, 12H, CH_2), 7.70 (br, 2H, aryl), 5.54 (s, 54H, ^{t}Bu), 4.65 (s, 36H, Me_2Si), 2.70 (br, 2H, aryl), −16.45 (br, 2H, aryl), −18.04 ppm (s, 12H, CH_2). IR (mineral oil) $\nu_{C\equiv C}$ 2060 cm^{-1}. Magnetic susceptibility (SQUID, 300 K): μ_{eff} = 4.45 μ_B. Anal. Calcd for $C_{58}H_{118}N_8Si_6U_2$: C, 44.31; H, 7.57; N, 7.12. Found: C, 44.24; H, 7.53; N, 6.96.

$[(NN'_3)_3U_3$(TEB)] (6). A solution of H_3TEB in 1 mL of pentane (0.020 g, 0.13 mmol) was added dropwise to a stirred solution of $[(bit\text{-}NN'_3)U]$ (0.306 g, 0.423 mmol) in 10 mL of pentane at −78 °C, and the resulting yellow-green solution was warmed to room temperature and stirred for 3 h. The solution was filtered, concentrated to about 2 mL under reduced pressure, and then cooled to −34 °C. After 8 h, a yellow-green microcrystalline precipitate was observed. The crude product was collected by filtration, dried in vacuo, and recrystallized from hot pentane to afford a yellow-green crystalline solid (0.243 g, 79%, based on H_3TEB). Single crystals suitable for X-ray analysis were grown from a concentrated pentane solution maintained at −34 °C for 8 h. Absorption spectrum (pentane) λ_{max} (ε_M): 292 (21000), 503 (11), 529 (114), 587 (44), 614 (23), 621 (23), 629 (20), 650 (16), 658 (17), 687 (198), 691 (177), 719 (33), 803 (8), 828 (13), 880 (12), 924 (13), 961 nm (9 L·mol^{-1}·cm^{-1}). IR (mineral oil): $\nu_{C\equiv C}$ 2054 cm^{-1}. Magnetic susceptibility (SQUID, 300 K): μ_{eff} = 5.45 μ_B. Anal. Calcd for $C_{84}H_{184}N_{12}Si_9U_3$: C, 43.50; H, 7.56; N, 7.22. Found: C, 43.14; H, 7.44; N, 6.82.

X-ray Structure Determinations. Structures were determined for the compounds listed in Table 1. Single crystals were coated with Paratone-N oil in the glovebox and mounted under a cold stream of dinitrogen gas. Single crystal X-ray diffraction data were acquired on a Bruker Kappa APEX II CCD diffractometer with $Mo_{K\alpha}$ radiation (λ = 0.71073 Å) and a graphite monochromator. Initial lattice parameters were obtained from a least-squares analysis of more than 100 reflections; these parameters were later refined against all data. None of the crystals showed significant decay during data collection. Data were integrated and corrected for Lorentz and polarization effects using SAINT, and semiempirical absorption corrections were applied using SADABS.[73] Space group assignments were based on systematic absences, E statistics, and successful refinement of the structures. Structures were solved by direct methods or Patterson maps and were refined with the aid of successive Fourier difference maps against all data using the SHELXTL 6.14 software package.[74] Thermal parameters for all atoms with Z > 3 were refined anisotropically, except for those disordered over multiple partially occupied sites in the structures of **4**·C_5H_{12} and **5**·C_5H_{12} and solvate molecules in **5**·C_5H_{12}. All hydrogen atoms were assigned to ideal positions and refined using a riding model with an isotropic thermal parameter 1.2 times that of the attached carbon atom (1.5 times for methyl hydrogens).

Data for **4**·C_5H_{12} were truncated to 1.0 Å resolution during integration because of weak scattering. In the structure of

(73) Sheldrick, G. M. *SADABS, A program for area detector absorption corrections*; Bruker AXS: Madison, WI.

(74) Sheldrick, G. M. *SHELXTL*, v 6.14; Bruker AXS: Madison, WI, 2004.

Table 2. Selected Bond Distances (Å) and Angles (deg) for Crystallographically (**1**−**5**) and Computationally Determined (**3**−**5**) Structures of the New Mono- and Dinuclear U(IV) Complexes

	1	**2**	**3**	**3** (calc)	**4**	**4** (calc)	**5**	**5** (calc)
U−C	2.604(3)	2.479(7)	2.480(4)	2.457	2.490(9)	2.447	2.31(2)	2.450
	2.562(2)	2.475(7)			2.443(9)	2.450	2.48(2)	
$U-N_{ax\ (amino)}$	2.6597(19)	2.668(5)	2.702(3)	2.668	2.693(6)	2.664	2.64(2)	2.667
		2.653(5)			2.673(6)	2.667	2.73(2)	
$U-N_{eq\ (amido)}$	2.2799(19)	2.285(5)	2.214(3)	2.222	2.207(6)	2.223	2.26(2)	2.223
		2.260(5)			2.214(6)	2.226	2.24(2)	
	2.293(2)	2.257(5)	2.220(3)	2.224	2.230(6)	2.226	2.26(2)	2.226
		2.284(5)			2.211(6)	2.224	2.18(2)	
	2.2437(19)	2.254(5)	2.245(3)	2.225	2.223(6)	2.227	2.12(2)	2.226
		2.263(5)			2.229(6)	2.227	2.28(2)	
C≡C	1.219(3)	1.210(9)	1.212(5)	1.229	1.215(10)	1.235	1.22(3)	1.236
	1.222(3)	1.219(9)			1.210(11)		1.42(3)	
U−C−C	177.8(2)	176.6(6)	160.9(4)	179.5	158.2(7)	179.6	177(2)	179.5
	169.1(2)	173.0(6)			170.2(7)		161(2)	179.6
$N_{ax}-U-C$	109.81(7)	165.06(19)	174.92(12)	178.0	174.7(2)	176.8	178.2(10)	177.3
	167.32(7)	161.08(19)			177.4(2)	177.2	177.4(8)	177.4
$N_{ax}-U-N_{eq}$	70.03(6)	68.03(17)	69.06(11)	67.7	69.5(2)	67.5	69.5(7)	67.5
		70.19(17)			69.41(12)		72.0(8)	
	70.06(6)	69.86(17)	69.26(11)	67.9	69.4(2)	68.0	68.1(8)	68.0
		70.20(16)			69.7(2)		69.5(7)	
	69.43(7)	68.70(16)	68.90(11)	67.9	70.2(2)	68.0	69.4(7)	68.0
		69.89(17)			69.9(2)		66.5(7)	
$N_{eq}-U-N_{eq}$	94.80(7)	100.7(2)	108.42(12)	106.2	107.0(2)	106.0	111.4(8)	106.0
		96.71(18)			107.1(2)	106.7	107.4(8)	107.3
	129.65(7)	124.96(19)	106.64(12)	106.8	111.0(2)	107.2	107.7(8)	106.7
		105.16(18)			107.2(2)	106.0	105.7(8)	106.7
	98.30(7)	121.86(19)	108.87(12)	107.0	111.6(2)	107.5	106.2(7)	106.0
		97.16(19)			107.8(2)	107.6	110.2(8)	107.1
U···U	n/a	13.0415(5)	n/a	n/a	9.2837(9)	11.297	12.9499(11)	13.065
U−O	n/a	2.503(4)	n/a	n/a	n/a	n/a	n/a	n/a
		2.571(4)						

4·C_5H_{12}, one of the Si^{t}BuMe$_2$ groups is disordered over two positions and refined to a 71:29 ratio. The methylene carbons (C29 and C30) of the ligand with the disordered Si group as well as all of the carbon atoms of the pentane solvate molecule were refined anisotropically but restrained to have the same U_{ij} parameters.

Data for **5**·C_5H_{12} were truncated to 0.9 Å resolution during integration because of weak scattering. In the structure of **5**·C_5H_{12}, two of the Si^{t}BuMe$_2$ groups are disordered over two positions and refined to 65:35 and 73:27 site occupancy ratios. All chemically equivalent atoms were restrained to have the same U_{ij} parameters. The space between the uranium complexes shows severe solvent disorder. One pentane solvate molecule was found in Fourier difference maps, and the thermal parameters of the carbon atoms were refined isotropically. SQUEEZE[75] was used to remove the remaining disordered components; approximately 0.25 equiv of pentane (per formula unit) are estimated to be present in the void space. The final residual structure factors for the structure of **5**·C_5H_{12} are high owing to extensive disorder and the accompanying poor quality of the data.

Refinement of matrix scans for crystals of **6** give a primitive orthorhombic cell with the following unit cell parameters: a = 18.5219(7), b = 22.2851(8), c = 28.0242(10) Å, and V = 11567(1) Å^3. A preliminary refinement of **6** confirms the expected cluster connectivity, but the diffraction data are not of sufficient quality to afford a complete X-ray analysis.

Selected bond distances and angles for crystals of compounds **1**−**5** are collected in Table 2. All other metric parameters can be found in the Supporting Information.

Magnetic Susceptibility Measurements. Magnetic susceptibility measurements were collected using a Quantum Design MPMS XL SQUID magnetometer. Direct current (DC) magnetic susceptibility data were collected at temperatures ranging from 2 to 300 K at an applied field of 0.1 T. Powdered microcrystalline samples (10−20 mg, ∼6−20 μmol) were loaded into gelatin capsules in the glovebox, inserted into a straw, and transported to the SQUID instrument under dinitrogen. AC magnetic susceptibility data were collected at temperatures ranging from 2 to 5 K at an applied field of 0.1 T with various AC frequencies. Powdered microcrystalline samples were loaded into gelatin capsules in the glovebox and suspended in Eicosane to prevent crystallites from torquing at high and/or alternating magnetic fields. Contributions to the magnetization from the gelatin capsule and the straw were measured independently and subtracted from the total measured signal. Data were corrected for diamagnetic contributions using Pascal's constants. Susceptibility data were fit with theoretical models using a relative error minimization routine (MAGFIT 3.1).[76] Reported coupling constants are based on exchange Hamiltonians of the form $\hat{H} = -2J(\hat{S}_i \cdot \hat{S}_j)$.

Other Physical Measurements. UV−visible absorption spectra were obtained in pentane or toluene solutions in an airtight glass cell of path length 1 cm on an Agilent 8453 spectrometer. ^{1}H NMR spectra were recorded using a Varian INOVA 500 MHz instrument, and the spectra were referenced internally using residual protio solvent resonances relative to tetramethylsilane (δ = 0 ppm). Infrared spectra were collected on a Thermo Nicolet 380 FTIR spectrometer as mineral oil mulls pressed between sodium chloride plates. EPR spectra were obtained on solid samples at ambient temperature using a continuous wave X-band Bruker EMX 200U instrument. Electrochemical measurements were conducted with a CH Instruments 1232A potentiostat/galvanostat, and the data were processed with CHI software (version 7.20). All experiments were performed in a glovebox using a 20 mL glass scintillation vial as the cell. The electrodes consisted of platinum wire microelectrode (0.250 mm diameter), platinum wire mesh counter, and Ag/Ag$^+$ reference electrodes. Solution concentrations employed during CV studies

(75) Spek, A. L. *J. Appl. Crystallogr.* **2003**, *36*, 7–13.

(76) Schmitt, E. A. Ph.D. Thesis, University of Illinois at Urbana-Champaign, **1995**.

were typically 3 mM for the uranium complex and 0.1 M for the [TBA][$B(Ar^F)_4$] electrolyte. All potentials are reported versus the $[Cp_2Fe]^{+/0}$ couple. Elemental analyses were performed by Columbia Analytical Services, Tucson, AZ (compounds **2**−**6**) or the University of California, Berkeley (compound **1**).

Electronic Structure Calculations. Spin unrestricted B3LYP hybrid density functional studies[77] were carried out on model complexes of **3**, **4**, and **5** where the Si^{t}BuMe$_2$ substituents are replaced by H atoms and geometries are optimized. Singlet states were described with broken symmetry representations. In a broken symmetry treatment, α and β orbitals of a given molecular orbital are allowed to be different, permitting the differential localization of α and β spin sets.[61] For $M_S = 0$ "singlet" states this model is not an eigenfunction of spin but is an admixture of spin states. The standard Noodleman spin projection formula ($J = (E_{HS} - E_{BS})/\langle S\rangle^2$) can be used to estimate spin−spin coupling constants, J.[78] This treatment has been demonstrated to reproduce spin−spin (J) coupling in transition metal complexes within a factor of 2.[79] The Stuttgart RSC 1997 basis and effective core potential was employed for U, which incorporates scalar relativistic effects and replaces 60 core electrons.[78−81] Linear dependency issues and SCF convergence was improved by deletion of the outermost zeta = 0.05 S, P, D, and F exponents. The 6-31g* basis sets were used for C, H, and N atoms.[82−84] All calculations were carried out in the G03 suite of electronic structure codes.[85] Selected bond distances and angles for the calculated structures are presented in Table 2. Coordinates for the calculated structures are provided in the Supporting Information.

Results and Discussion

Syntheses and Characterizations of [(NN′$_3$)U] Acetylide Complexes. Several monomeric synthons avail themselves for the preparation of pentacoordinate U(IV) species. Scott and co-workers have shown that the [(NN′$_3$)UCl] complex can undergo ligand substitution with a variety of lithiated ligands via salt metathesis.[66] However, in our hands the apparent 1:1 combination of [(NN′$_3$)UCl] with lithium phenylacetylide does not yield the expected pentacoordinate complex, but instead produces a hexacoordinate species, [(NN′$_3$)U(CCPh)$_2$(Li·THF)] (**1**) as the only isolable product (eq 1).

$$[(NN'_3)UCl]\cdot x\mathrm{THF} + 2\mathrm{Li(CCPh)} \rightarrow [(NN'_3)U(CCPh)_2(\mathrm{Li}\cdot\mathrm{THF})] + \mathrm{LiCl} \quad (1)$$

Adventitious THF present in the unsublimed U(IV) starting material changes the stoichiometry of the reaction, and lithium ion coordination to the phenyl acetylide ligands likely drives formation of **1** over the expected monoarylacetylide compound. Rationalization of the reaction conditions by doubling the amount of added lithium phenylacetylide and performing the reaction with an excess of THF allows for a greater isolated yield of the hexacoordinate U(IV) bis-arylacetylide complex.

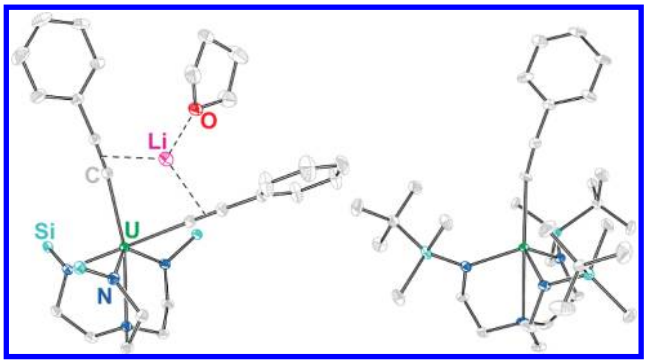

Figure 1. Crystal structures of the U(IV) arylacetylide complexes in compounds **1** (left) and **3** (right), rendered with 40% ellipsoids. Green, dark blue, light blue, red, purple, and gray ellipsoids represent U, N, Si, O, Li, and C atoms, respectively. Hydrogen atoms are omitted for clarity, and the ^{t}BuMe$_2$ groups have been removed from the Si atoms in **1** for a clearer display of the coordination geometry about the uranium center.

The X-ray analyses of single crystals of **1** reveal two different polymorphs depending on the reaction conditions ($P\bar{1}$ from 1:1 and $P2_1/c$ from 1:2 stoichiometry). Metric parameters for the complexes in both polymorphs are essentially identical; the structures differ only in the relative orientation of the complexes within the unit cells. The thermal ellipsoid representation of the monoclinic polymorph of **1** is shown in Figure 1; see the Supporting Information for the triclinic structure. The uranium is ligated by three amido nitrogens, one amine nitrogen, and two phenylacetylide carbon atoms in η^1 fashion. The (NN′$_3$) fragment is unsymmetrically oriented with respect to the metal center, resulting in a wider range of "flap" dihedral angles N_{ax}−U−N_{eq}−Si (137−163°) than is normally observed for virtually all other compounds containing the [(NN′$_3$)U] fragment (131−137°).[63] However, the range of dihedral angles in **1** is similar to that reported by Scott and co-workers for the U(V) oxo-bridged complex [(*bit*-NN′$_3$)$_2$U$_2$(μ-O)] (132−177°).[63] The ligands form a distorted octahedral first coordination sphere about the metal center, as evidenced by the $\sum$ parameter (177.71), which is the sum of the deviations from 90° of the twelve *cis* φ angles in the coordination sphere ($\sum = \sum_{i=1}^{12}|90 - \varphi_i|$).[86] The two acetylide bridges are nearly linear, with U−C−C angles of 169.1(2) and 177.8(2)°. This contrasts with the only other structurally characterized U(IV) aryl acetylide complex, [(NN′$_3$)U(CCPhMe)], a pentacoordinate U(IV) complex that shows a U−C−C angle of 156.4°.[63] In the structure of **1**, the lithium ion is coordinated by THF in an η^1 mode, and by the acetylides in a π fashion; the latter coordination mode may help explain the observed linearity of the U−C−C linkages.

The absorption spectrum of **1** (Supporting Information, Figure S7) contains only one feature at 686 nm. While spectral features which would normally mark the presence of a U(IV) ion in solution are absent, the position (686 nm) and molar absorptivity (95 L·mol^{-1}·cm^{-1}) of the singular absorption maximum observed are similar to other

(77) Becke, A. D. *J. Chem. Phys.* **1993**, *98*, 5648–5652.
(78) Noodleman, L.; Davidson, E. R. *Chem. Phys.* **1986**, *109*, 131–143.
(79) Hart, J. R.; Rappe, A. K.; Gorun, S. M.; Upton, T. H. *J. Phys. Chem.* **1992**, *96*, 6255–6263.
(80) Noodleman, L. *J. Chem. Phys.* **1981**, *74*, 5737–5743.
(81) Kuechle, W.; Dolg, M.; Stoll, H.; Preuss, H. *Mol. Phys.* **1991**, *74*, 1245–1263.
(82) Ditchfield, R.; Hehre, W. J.; Pople, J. A. *J. Chem. Phys.* **1971**, *54*, 724−728.
(83) Hehre, W. J.; Ditchfield, R.; Pople, J. A. *J. Chem. Phys.* **1972**, *56*, 2257−2261.
(84) Binkley, J. S.; Pople, J. A.; Hehre, W. J. *J. Am. Chem. Soc.* **1980**, *102*, 939–947.
(85) Frisch, M. J. et al. *Gaussian 03*; Gaussian, Inc.: Wallingford, CT, 2004.
(86) Guionneau, P.; Marchivie, M.; Bravic, G.; Letard, J. F.; Chasseau, D. *J. Mater. Chem.* **2002**, *12*, 2546–2551.

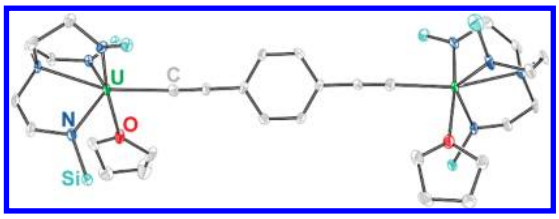

Figure 2. Crystal structure of the dinuclear complex in compound $2\cdot THF\cdot C_5H_{12}$, rendered with 40% ellipsoids. Green, dark blue, light blue, red, and gray ellipsoids represent U, N, Si, O, and C atoms, respectively. ^{t}BuMe$_2$ groups have been removed from the Si atoms for a clearer display of the coordination geometry about the uranium center. Hydrogen atoms and solvent molecules are omitted for clarity.

pentacoordinate U(IV) complexes containing the (NN'_3) ligand.[66,71,87]

Whereas the reaction of $[(NN'_3)UCl]$ with lithium phenylacetylide yields a bis-phenylacetylide complex, its combination with 0.5 equiv of a ditopic aryl acetylide such as Li_2(*p*-DEB) results in the formation of a dinuclear U(IV) complexes via eq 2:

$$2[(NN'_3)UCl]\cdot x\text{THF} + Li_2(p\text{-DEB}) \rightarrow [(NN'_3)_2U_2(p\text{-DEB})(\text{THF})] + 2\text{LiCl} \quad (2)$$

Unlike the formation of **1**, only one acetylide interacts with each U(IV) ion; however, the presence of adventitious THF nevertheless provides at least some hexacoordinate U(IV) species in the final product. Uranium complexes are quite oxophilic,[88] and consistent with the formation of complex **1**, the triamidoamine groups are not sufficiently sterically encumbering to prevent the coordination of a sixth ligand. Thus, hexacoordinate geometry is observed in the solid state structure of $[(NN'_3)_2U_2(p\text{-DEB})(THF)_2]$ ($2\cdot$THF), as determined by X-ray analysis (Figure 2). Again, the $[(NN'_3)U]$ fragment is asymmetrically oriented, as measured by the dihedral angles $N_{ax}-U-N_{eq}-Si$ ranging from 132 to 176°.[63] The U−O distances (2.583(4) and 2.571(4) Å for U1−O1 and U2−O2, respectively) are similar to those reported for other crystallographically characterized U(IV) THF adducts.[87,89−92] The THF solvent molecules are rotated by approximately 90° with respect to each other. The η^1-bound acetylide in **2** links the uranium centers in a nearly linear fashion with U−C−C angles of 173.0(6) and 176.6(6)°. The uranium centers in $2\cdot$THF sit in distorted octahedrons as measured by their respective $\sum$ parameters (175.21° for U1 and 191.78° for U2).[86] The (NN'_3) fragments in $2\cdot$THF are rotated by approximately 90° with respect to each other.

Whereas the crystal structure of $2\cdot THF\cdot C_5H_{12}$ clearly shows two THF molecules per complex, the elemental analysis data obtained for bulk **2** indicate that approximately one THF molecule is absent in the bulk samples. As will be discussed in more detail below, the "hexacoordinate" **2** and the pentacoordinate **5** are found to have virtually identical spectroscopic properties.

Scheme 1. Synthesis of Complexes **3**−**6**[a]

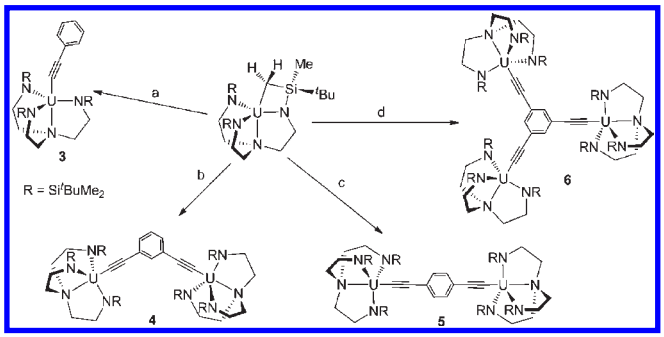

[a] a = phenylacetylene, b = *m*-H_2DEB, c = *p*-H_2DEB, and d = H_3TEB. All reactions were carried out in pentane at −78 °C.

Alternatively, the monodeprotonated complex [(*bit*-NN'_3)U] can serve as an excellent precursor for reactions with free acetylenes, also previously demonstrated by Scott and co-workers.[63] As shown in Scheme 1, the triamidoamine ligand can be reprotonated by the acetylene, and the acetylide anion formed in situ can bind to the cationic U(IV) center. In our hands, the combination of the orange-brown [(*bit*-NN'_3)U] with 1 equiv of phenylacetylene allows for the preparation of the yellow-green pentacoordinate U(IV) monoacetylide complex (**3**) in good yield.

The crystal structure of monomeric **3**, determined from crystals grown at −34 °C from a saturated pentane solution (Figure 1), is very similar to the previously reported $[(NN'_3)U(CCPhMe)]$ complex.[93] The triamidoamine ligand adopts a typical trigonal pyramidal geometry around the uranium center in **3**. Although not imposed crystallographically, the ligand is essentially 3-fold symmetric about the U center, as measured by the dihedral angles $N_{ax}-U-N_{eq}-Si$ (131−137°). The acetylide ligand binds the U(IV) ion in an η^1 fashion, but shows a bent configuration unlike those of the nearly linear acetylides in the hexacoordinate complex **2** (U−C−C angle 160.9(4)°). This bending is similar to Scott's pentacoordinate complex, where it was suggested that the alkynyl uranium fragment bends to allow for increased U−C π-overlap.[63] Density functional theory (DFT) calculations (discussed below) reveal that bending the U−C−C bond angle from 180° to 160° only slightly perturbs the energy of the complex, implying that intermolecular packing forces may represent significant contributors to the observed bond angles.

Utilizing the same revision to the synthetic procedure as described in the synthesis of **3**, we find that mixing [(*bit*-NN'_3)U] with the appropriate acetylenes leads to di- and trinuclear complexes in which the U(IV) center is pentacoordinate (Scheme 1). In this manner, we have prepared the di- and trinuclear U(IV) ethynylbenzene complexes $[(NN'_3)_2U_2(m\text{-DEB})]$ (**4**), $[(NN'_3)_2U_2(p\text{-DEB})]$ (**5**), and $[(NN'_3)_3U_3(TEB)]$ (**6**) in good yields. Crystal structures for the dinuclear compounds **4** and **5** are depicted in

(87) Ball, R. G.; Edelmann, F.; Matisons, J. G.; Takats, J.; Marques, N.; Marcalo, J.; Dematos, A. P.; Bagnall, K. W. *Inorg. Chem. Acta* **1987**, *132*, 137–143.
(88) Gorden, A. E. V.; Xu, J. D.; Raymond, K. N.; Durbin, P. *Chem. Rev.* **2003**, *103*, 4207–4282.
(89) Charpin, P.; Nierlich, M.; Vigner, D.; Lance, M.; Baudin, C. *Acta Crystallogr.* **1988**, *44*, 255–257.
(90) Gaunt, A. J.; Scott, B. L.; Neu, M. P. *Inorg. Chem.* **2006**, *45*, 7401–7407.
(91) Salmon, L.; Thuery, P.; Asfari, Z.; Ephritikhine, M. *Dalton Trans.* **2006**, 3006–3014.
(92) Salmon, L.; Thuery, P.; Ephritikhine, M. *Chem. Commun.* **2006**, 856–858.
(93) Boaretto, R.; Roussel, P.; Kingsley, A. J.; Munslow, I. J.; Sanders, C. J.; Alcock, N. W.; Scott, P. *Chem. Commun.* **1999**, 1701–1702.

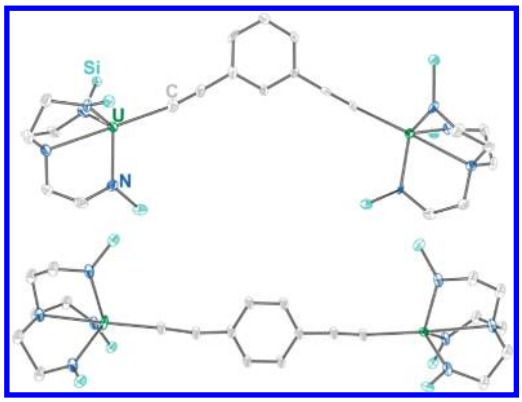

Figure 3. Crystal structures of the dinuclear complexes in compounds $4\cdot C_5H_{12}$ (top) and $5\cdot C_5H_{12}$ (bottom), rendered with 40% ellipsoids. Green, dark blue, light blue, and gray ellipsoids represent U, N, Si, and C atoms, respectively. ^{t}BuMe$_2$ groups have been removed from the Si atoms for a clearer display of the coordination geometry about the uranium center. Hydrogen atoms and solvent molecules are omitted for clarity. One and two of the SiMe$_2{}^t$Bu groups are disordered over two positions for $4\cdot C_5H_{12}$ and $5\cdot C_5H_{12}$, respectively; only one orientation is shown for clarity. See Supporting Information, Figures S24 and S25 for disordered components.

Figure 3. Crystals of trinuclear **6** diffract sufficiently to confirm the expected cluster connectivity, but the diffraction data are not of sufficient quality to provide a complete X-ray analysis. As with compound **3** (see Table 2 for comparisons of bond distances and angles), the [(NN′$_3$)U] adopts its usual orientation, with dihedral angles of 132−142° and 136−145° for meta- and para-bridged **4** and **5**, respectively. Interestingly, one of the U−acetylide linkages in meta-bridged **4** is significantly more linear than the other (U−C−C angle of 158.2(7)° versus 170.2(7)°). Fourier difference maps do not indicate any evidence for crystallographic disorder present in the structure of **4**. Rather, the different U−C−C bond angles observed could be due to a competition between (NN′$_3$) sterics, which would favor linear U−C−C linkages, and π-overlap of the acetylide and U(IV) ion, similar to that observed in the structure of the monomeric complex **3**. The (NN′$_3$) fragments in meta-bridged **4** are rotated by approximately 60° with respect to each other. In para-bridged **5**, the (NN′$_3$) fragments are not rotated with respect to each other and can be related by a non-crystallographic mirror plane.

We have characterized all the ethynylbenzene-bridged species by FT-IR and UV−visible spectroscopic techniques (Supporting Information, Figures S1−S12). The fingerprint region of the IR is nearly identical to those reported for most of the structurally characterized compounds containing the [(NN′$_3$)U] fragment.[63,64,66,94] The electronic absorption spectra of uranium compounds represent a good indicator for the oxidation state of the metal ion; and the spectra of complex **2** and compounds **4**−**6** are consistent with an assignment of U(IV), in agreement with other reported [(NN′$_3$)U]-containing compounds.[95] Interestingly, the UV−visible spectra of **2** and **5** in toluene are similar; they also display similar

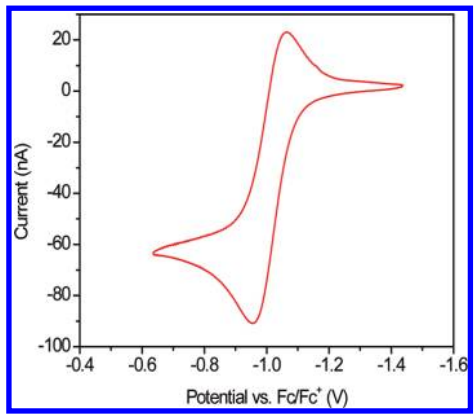

Figure 4. Electrochemical behavior for **3** in static solution recorded in 0.1 M solution of [TBA][BAr$^F{}_4$] in *o*-difluorobenzene at ambient temperature with a 0.250 mm diameter platinum wire microelectrode.

infrared spectra. While these could indicate that the coordination environment of the uranium center does not have a discernible effect on electronic properties, more likely these results point to THF solvate loss in solution. Thus, crystals of $2\cdot THF\cdot C_5H_{12}$ show two THF molecules, but bulk **2** contains only one, and dissolved **2** is spectroscopically identical to **5**, which contains no THF solvate.

Oxidation of the Pentacoordinate U(IV) Arylacetylide Complexes. Efforts to produce unambiguously paramagnetic U-containing assemblies, either by oxidations or reductions of **2** and **4**−**6** that may lead to U(V) or U(III) species, respectively, yield mixed results. Cyclic voltammetry experiments performed on the monomeric phenylacetylide complex **3** in *o*-difluorobenzene show a well-defined, reversible wave centered at −1.02 V versus Fc$^+$/Fc (Figure 4). This process is assignable to an oxidation of the neutral compound to a formally U(V) species, and is supported by an agitation experiment whereby the voltammogram is collected while stirring the sample (Supporting Information, Figure S13). This is comparable to results reported by Kiplinger and co-workers for [(C$_5$Me$_5$)$_2$U(=N−Ar)(X)] (X = F, Cl, Br, I), where reversible couples ranging between −1.21 and −1.84 V versus Fc$^+$/Fc are observed.[96] While the cyclic voltammograms suggest a reversible U(IV/V) redox couple on the time scale of the experiment (scan rate of 50 mV/s), initial attempts to isolate oxidized complexes by chemical oxidation with [FeCp*$_2$](BAr$^F{}_4$) have not been successful. Infrared spectra obtained on the products of oxidation attempts show no shift in the acetylide resonance, contrary to what would be expected if a change in uranium oxidation state occurred. In addition, crystals isolated from the oxidation attempts were determined to be [(C$_5$Me$_5$)Fe(C$_5$Me$_4$CH$_2$)](BAr$^F{}_4$).[97]

Attempts to obtain cyclic voltammograms on compounds **2**, **4**, **5**, and **6** under similar conditions have proven more difficult. Although experimental conditions have been systematically varied (including solvents, scan rates, and working electrodes), in all instances, only ill-defined waves are observed (Supporting Information, Figure S14),

(94) Roussel, P.; Boaretto, R.; Kingsley, A. J.; Alcock, N. W.; Scott, P. *J. Chem. Soc., Dalton Trans.* **2002**, 1423–1428.
(95) Schelter, E. J.; Veauthier, J. M.; Graves, C. R.; John, K. D.; Scott, B. L.; Thompson, J. D.; Pool-Davis-Tournear, J. A.; Morris, D. E.; Kiplinger, J. L. *Chem.—Eur. J.* **2008**, *14*, 7782–7790.
(96) Graves, C. R.; Vaughn, A. E.; Schelter, E. J.; Scott, B. L.; Thompson, J. D.; Morris, D. E.; Kiplinger, J. L. *Inorg. Chem.* **2008**, *47*, 11879–11891.
(97) Kreindlin, A. Z.; Dolgushin, F. M.; Yanovsky, A. I.; Kerzina, Z. A.; Petrovskii, P. V.; Rybinskaya, M. I. *J. Organomet. Chem.* **2000**, *616*, 106–111.

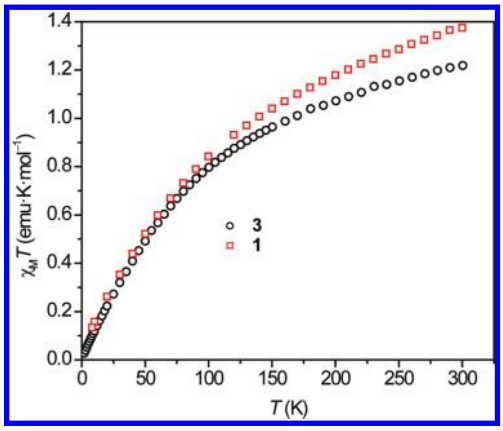

Figure 5. Temperature dependence of the magnetic susceptibility for compounds $[(NN'_3)U(CCPh)_2(Li\cdot THF)]$ (**1**) and $[(NN'_3)U(CCPh)]$ (**3**), obtained at a measuring field of 1000 G.

suggesting the occurrence of multielectron processes and/or the decomposition of the original species. It is also possible that the complicated nature of the cyclic voltammograms could be due to electronic communication between the uranium centers via the bridging ligand.

Magnetic Properties of the U(IV) Complexes. The temperature dependence of the magnetic susceptibility (2−300 K) for each uranium-acetylide complex was characterized by SQUID magnetometry (Figures 5 and 6, also Supporting Information, Figures S15−S17), and MAGFIT[76] was used to fit the subtracted paramagnetic susceptibility data (vide infra) to a simple spin Hamiltonian with one exchange parameter J (black traces in Figure 6 and Supporting Information, Figures S15−S17). Fitted parameters are listed in Table 3.

Magnetic Susceptibilities of Monomeric Complexes 1 and 3. The temperature dependencies of the magnetic susceptibility, $\chi_M T$, for the monomeric U(IV) arylacetylide complexes **1** and **3** are shown in Figure 5. The room temperature $\chi_M T$ values for **1** and **3** (1.37 and 1.18 emu·K·mol^{-1}, respectively) are comparable to those of other reported complexes containing U(IV) in a low symmetry ligand field and are consistent with the presence of paramagnetic state(s) at room temperature.[49,94,98] Upon decreasing the temperature, higher-energy Stark sublevels begin to depopulate, resulting in a subsequent decrease in the magnitude of the total angular momentum vector. This phenomenon leads to a variation in the thermal population of the many states that are energetically comparable to the ground state.[11] The physical manifestation of this decrease in the angular momentum is evident by the decrease in the observed magnetic susceptibility. As can be seen in a plot of $\chi_M T$ versus T for **1**, a gradual decrease to 0.93 emu·K·mol^{-1} at 120 K occurs, followed by a sharper decrease to 0.13 emu·K·mol^{-1} at 8 K. Similarly, as the temperature is reduced to 160 K, $\chi_M T$ for **3** reveals a gradual decrease to 0.99 emu·K·mol^{-1}, followed by a sharper decrease to 0.03 emu·K·mol^{-1} at 2 K. The behavior of the hexacoordinate **1** can be interpreted as a ground state diamagnetic f^2 species, which is paramagnetic at room temperature because of spin−orbit coupling, temperature-independent

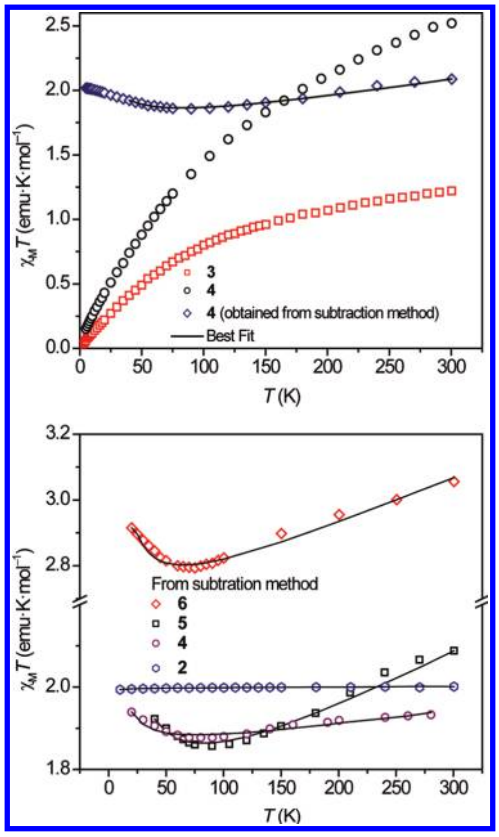

Figure 6. Top: temperature dependence of the magnetic susceptibility for compounds **3** and **4**, obtained at a measuring field of 1000 G; and fit of the data obtained from the subtraction method for **4**, see text for details of the fitting procedures. Bottom: solid lines give best fits to the data obtained from the subtraction method for complexes **2**, **4**, **5**, and **6**; see text for details of the data correction procedures.

Table 3. Tabulated MAGFIT Results for Compounds $[(NN'_3)]_2U_2(p\text{-DEB})(THF)]$ (**2**), $[(NN'_3)_2U_2(m\text{-DEB})]$ (**4**), $[(NN'_3)_2U_2(p\text{-DEB})]$ (**5**), and $[(NN'_3)_3U_3(TEB)]$ (**6**)

	2	**4**	**5**	**6**
J (cm^{-1})	−0.05	4.76	2.75	1.11
g	1.99	1.80	1.89	1.84
TIP (×10^{-6} emu)	5	1435	860	1473
relative error	0.19	0.18	0.08	0.17

magnetism (TIP), and thermal population of paramagnetic excited states. A poorly isolated singlet ground state is not atypical for complexes with $5f^2$ valence configurations;[99−101] further, it is well-known that an octahedral ligand field will produce a diamagnetic ground state for a $5f^2$ electronic configuration.[59] Although the pentacoordinate species **3** also displays magnetic properties which appear to be consistent with a non-magnetic ground state,[102−104] there seems to be less influence from TIP than

(98) Spirlet, M. R.; Rebizant, J.; Apostolidis, C.; Dornberger, E.; Kanellakopulos, B.; Powietzka, B. *Polyhedron* **1996**, *15*, 1503–1508.

(99) Siddall, T. H. *Theory and Applications of Molecular Paramagnetism*; Wiley: New York, 1976.

(100) Kanellakopulos, B. *Organometallics of the f-Elements*; D. Reidel Pub. Co.: Dordrecht, The Netherlands, 1978.

(101) Edelstein, N. M.; Lander, G. H. *The Chemistry of the Actinide and Transactinide Elements*; Morss, L. R., Edelstein, N. M., Fuger, J., Eds.; Springer: Dordrecht, The Netherlands, 2006; Vol. *4*, Chapter 20.

(102) Almond, P. M.; Deakin, L.; Porter, M. J.; Mar, A.; Albrecht-Schmitt, T. E. *Chem. Mater.* **2000**, *12*, 3208–3213.

(103) Kiplinger, J. L.; Pool, J. A.; Schelter, E. J.; Thompson, J. D.; Scott, B. L.; Morris, D. E. *Angew. Chem., Int. Ed.* **2006**, *45*, 2036–2041.

(104) Schelter, E. J.; Morris, D. E.; Scott, B. L.; Thompson, J. D.; Kiplinger, J. L. *Inorg. Chem.* **2007**, *46*, 5528–5536.

observed for **1**. Overall, the foregoing results imply that coordination geometry differences impart only minor impacts on the magnetic properties of these [(NN'_3)U]-containing complexes.

Magnetism of Di- and Trinuclear Species 2, 4−6. The temperature dependence of the magnetic susceptibility for dinuclear "hexacoordinate" complex **2** is shown in Supporting Information, Figure S15. The room temperature $\chi_M T$ value for **2** (1.40 emu·K·mol^{-1} per U(IV) ion) is comparable to that of other reported complexes with U(IV) in a low symmetry ligand field.[49,94,98] It is important to note that $\chi_M T$ drops as the temperature approaches zero to a minimum of 0.04 emu·K·mol^{-1} at 2 K. Again, this may be due to "octahedral" geometry, similar to the description of the magnetic properties of **1**. However, the drop is not linear like **1**, perhaps related to the fact that the 6-coordinate geometry is quite distorted from a perfect octahedron. The construction of a Weiss plot for **2** (Supporting Information, Figure S18) yields a θ value of −180 K with a Curie constant (C) of 4.44 cm^3·K·mol^{-1}. A complicating factor in magnetic interpretation for the compound is the potential loss of some THF from ground up bulk samples of this compound. In fact, if the mass of 1 equiv of THF is removed from **2**, the adjusted susceptibility data virtually overlay the data for para-bridged **5** (vide infra).

Although complexes **4−6** display quite different coordination geometries from the crystal of **2**·THF, their magnetic properties appear to be quite similar on a per U(IV) basis. The temperature dependence of the magnetic susceptibility, $\chi_M T$, for the meta-bridged dinuclear complex **4** is shown in Figure 6; those for para-bridged **5** and TEB-bound **6** can be found in the Supporting Information (Figures S16, and S17, respectively; Supporting Information, Figure S18 reveals Weiss constant determinations). The room temperature $\chi_M T$ value for **4** (1.26 emu·K·mol^{-1} per U(IV) ion) is in the range of other literature values for paramagnetic U(IV) ions in low symmetry ligand fields.[49,94,98] Similar to the behavior of **2**, $\chi_M T$ approaches zero as the temperature is reduced, which appears to be consistent with a non-magnetic ground state.[102−104] This is inconsistent with the simple ligand-field diagram for an f^2 ion in trigonal bipyramidal complex geometries; however, it must be noted that spin−orbit coupling was not included in the group theoretical analysis.

However, when we perform a precedented subtraction scheme[11] on the susceptibility data for complexes **2**, **4**, **5**, and **6**, the adjusted data reveal evidence of net intramolecular exchange interactions.[50,105] Here, the discussion is focused on the data interpretation for meta-bridged **4**, but is applicable to the magnetic interpretations for the other multinuclear complexes **2**, **5**, and **6**. At each temperature, two times the paramagnetic susceptibility of the mono-acetylide species **3** (three times in the case of trinuclear **6**) are subtracted from the corresponding paramagnetic susceptibility of the dinuclear meta-bridged complex **4** to remove any contribution from the spin−orbit coupling present in the U(IV) ions. To this value is added the contribution expected for two $S = 1$ ions (i.e., $\chi_M T = 1.00$ for $g = 2.00$). In the case where no communication between the metal centers is occurring, a plot of the obtained values versus temperature is expected to form a line with zero slope at a $\chi_M T$ value of 2.00 emu·K·mol^{-1} (assuming $g = 2.00$).[50,53,65,101] However, the resulting blue traces (Figure 6, Supporting Information, Figures S15−S17) do possess some curvature, suggesting the presence of U−U magnetic interactions. While this method of data treatment only allows an estimation of the lower limit to any exchange interactions (since spin−orbit interactions have been removed), MAGFIT estimates the magnetic exchange in meta-bridged **4** to be weakly *ferro*magnetic, with $J = 4.76$ cm^{-1}. There are scant comparisons available in the literature. The coupling in [$(MeC_5H_4)_6U_2(\mu$-1,4-$N_2C_6H_4)$] was reported by Andersen and co-workers to be significantly stronger and antiferromagnetic, ($J = -19$ cm^{-1});[57] however it must be noted that this represents coupling between U(V) centers. Meanwhile, coupling between U(IV) and Ni(II) ions in {(cyclam)Ni[$(\mu$-Cl)U$(Me_2Pz)_4]_2$} using the above-mentioned subtraction scheme yields a J value of 2.8 cm^{-1};[50] although the structure is not similar to the compounds presented here, the result shows that coupling in the single wavenumber range is not unexpected. Finally, coupling of Fe(III) ions through the *m*-DEB bridge is ferromagnetic, albeit significantly stronger than that observed in the meta-bridged dinuclear complex **4** ($J = 65$ cm^{-1}).[67]

Interestingly, fits to the data for para-bridged **5** and trinuclear complex **6** (Table 3) also indicate weak ferromagnetic coupling, although the J couplings are weaker (2.75 and 1.11 cm^{-1}, respectively) than that determined for **4**. Note that g values determined from the fitting procedure are consistent with other reported U(IV) complexes.[49,50] In an attempt to compare experimental and fitted g values, preliminary room temperature electron paramagnetic resonance (EPR) data were collected for meta-bridged **4**; however, no signal was obtained, which is not unexpected for an integer spin system ($S = 1$ or 0). Data derived from best fits for "hexacoordinate" dinuclear complex **2** are also presented in Table 3, but the determined parameters are less reliable owing to the lack of a suitable monomeric hexacoordinate U(IV) complex for use in the data adjustment scheme, as well as uncertainty about the coordination geometry in bulk samples of **2**.

Indeed, this exemplifies a general concern about the potential for measurement errors to propagate in the course of applying the subtraction scheme. Regarding the reproducibility of data, we have analyzed multiple samples of the mono- and multinuclear complexes, both within a batch and between different preparations, and obtain the same raw data in all cases. With respect to electronic differences between the mono- and multinuclear complexes (**3** and **4−6**, respectively) it is possible that the observed curvature in the $\chi_M T$ versus T plots is an artifact, but the structural similarities between the complexes argues against this. Finally, fits to the corrected data give the same values, even when the initial guesses for J and g are varied significantly. Thus, we argue that the temperature dependence of the corrected susceptibilities represent real albeit qualitative evidence of magnetic coupling operative between U(IV) centers.

(105) Salmon, L.; Thuery, P.; Riviere, E.; Girerd, J. J.; Ephritikhine, M. *Chem. Comm.* **2003**, 762–763.

On the basis of analogy with transition metal analogues,[67,68] we would expect antiferromagnetic coupling for paramagnetic species bridged by *p*-DEB and ferromagnetic exchange for di- and trinuclear complexes bridged by *m*-DEB and TEB, respectively. In support of this, antiferromagnetic coupling is observed in Andersen's para-substituted imido bridged U^{V}_{2} species.[57] Thus, while the results of the subtraction procedure may appear reasonable for the meta-linked complexes **4** and **6**, we might expect *antiferro*magnetic coupling for the *p*-DEB-bridged **5**. That this is not operative suggests that the particular bridging geometry may only have a small effect on the type of coupling in these U(IV) complexes. We note, however, that the geometry and nuclearity do appear to have an effect on the strength of the coupling (Table 3). First, the meta-linked **4** exhibits a *J* value twice as large as that determined for **5**. Second, comparison of the magnetic data for **4** and **6** shows that increasing the number of uranium centers results in a smaller coupling constant. Similar effects have been observed in cyanide-bridged transition metal complexes, where increased nuclearity distributes spin density over a larger area, resulting in weaker coupling.[106]

An important part of this discussion is that we must fully consider the possibilities that intermolecular pathways (H-bonding, U−U interactions, and close contacts) could contribute to the observed magnetic properties, and confirm that they are not significant contributors. There were no significant contacts in compounds **1**−**6**, other than weak van der Waals interactions, that would allow for any obvious pathways for magnetic communication to occur (see Supporting Information). In compounds **1**−**6**, the shortest intermolecular U···U distance was found in **4** with a distance of 8.9261(5) Å. The shortest intramolecular U···U interaction was also found in **4** with a distance of 9.2837(9) Å. None of these contacts portend significant contributions to the observed magnetism, thus lending further support to our assertion that any residual magnetism in these complexes is due to intramolecular communication between the uranium centers.

AC susceptibility measurements carried out on meta-bridged **4** do not show a change in the out-of-phase signal, even at switching frequencies of ∼1500 Hz (Supporting Information, Figure S26). Thus, regardless of coupling considerations, at least meta-bridged **4** does not show properties consistent with SMM behavior.

Theoretical Considerations. To gain deeper insight into the complex magnetic behavior, we carried out geometry-optimized Stuttgart/6-31g* B3LYP hybrid DFT calculations on model systems where the $Si^{t}BuMe_2$ substituents in the NN'_3 ligand are replaced by H atoms and relativistic effects are explicitly included in the uranium effective core potential. The structure obtained from the geometry optimization of a mononuclear model of **3**, $[N(CH_2CH_2NH)_3U(CCH)]$, compares well with the crystal structure of **3**, although one difference is that the U−C−C linkage is linear in the model complex. Computations carried out as a function of the U−C−C angle (Supporting Information, Figure S23) address the observation of both bent and linear U−C−C linkages in the isolated complexes **1**−**6**. The calculations show that bending the U−C−C angle from 180° to 160° only increases the energy by 0.5 kcal/mol for both the ground state triplet and lowest energy excited state singlet. The harmonic curve in Supporting Information, Figure S23 demonstrates that, as is typical of *sp* hybridized carbon, the bending potential is more quartic than harmonic in character.

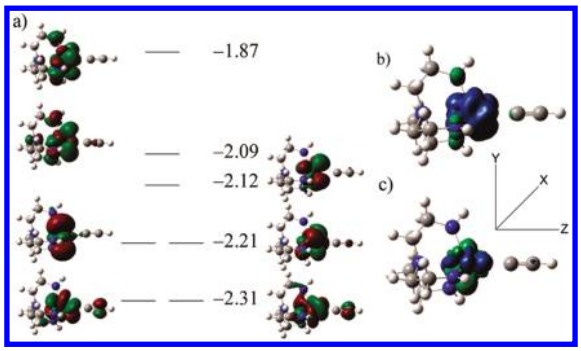

Figure 7. (a) Average field fragment molecular orbital diagram for $[N(CH_2CH_2NH)_3U(CCH)]$, relative energies are provided on an eV scale. (b) Net spin density plot of the ground state triplet. (c) Net spin density plot of the lowest "singlet" broken symmetry state. Blue surfaces correspond to net α spin density and green to net β spin density.

A conventional (spin−orbit coupling omitted) study on the model for **3** yields a triplet ground state with two electrons in quasi degenerate, singly occupied f orbitals—consistent with the group theoretic analysis.[58] The calculated f orbitals are mixtures of the 5f general set;[107] the occupied orbitals that would have π overlap with the acetylide ligand most closely resemble f_{xz^2} and f_{yz^2} (Figure 7). The lowest $M_S = 0$ "singlet" state is one wherein the two singly occupied orbitals are "singlet coupled" via a broken symmetry solution. To obtain the relative energies of the set of 7 f orbitals as well as to obtain the character of these frontier orbitals, an average field computation was carried out wherein the two triplet-coupled electrons are evenly distributed over the 7 f orbitals. Only the two lowest energy orbitals, the ones occupied in the conventional triplet study, show net orbital overlap with the π-type orbitals on the bound acetylide. Nevertheless, net spin density plots for the ground state triplet and lowest excited state singlet (Figure 7b and c) show that negligible spin density is found on the acetylide. As is visually evident in Figure 7, the 7 frontier orbitals are dominantly 5f in character. The largest d coefficient in any of the seven frontier orbitals is only 0.118. For the two lowest energy average field orbitals the largest d function coefficient is 0.029.

The triplet state is lower in energy than the broken symmetry solution by 8.4 kcal/mol. Given a U(IV) spin−orbit coupling parameter of roughly 6.3 kcal/mol,[58] however, the triplet and singlet states should strongly mix, resulting in a $j = 0$ ground state. This is consistent with the observed magnetic properties of **3**, where a paramagnetic complex at room temperature becomes "non-magnetic" as the temperature is reduced.

For model species based on the dinuclear complexes **4** and **5**, a broken symmetry model was used to construct

(106) Shores, M. P.; Sokol, J. J.; Long, J. R. *J. Am. Chem. Soc.* **2002**, *124*, 2279–2292.

(107) Chiu, Y. N.; Wang, F. E. *Theor. Chim. Acta* **1985**, *68*, 179–195.

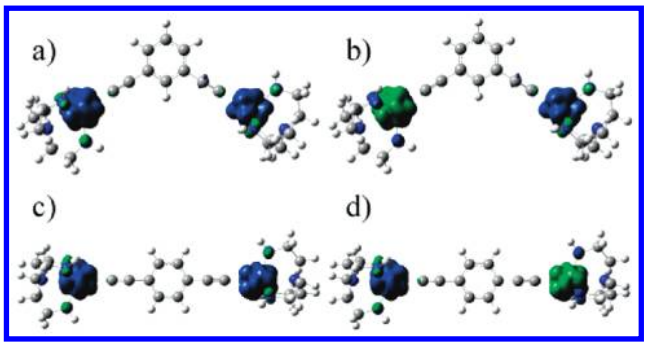

Figure 8. Net spin density plots for *m*- and *p*-DEB-bridged dinuclear species based on **4** and **5**. Blue surfaces correspond to net α spin density and green to net β spin density. Triplets are displayed in a and c, and singlet (broken symmetry) wave functions are shown in b and d.

the antiferromagnetically coupled low spin state, and J was computed to be 1.6 and -0.1 cm^{-1} for the meta- and para-bridged complexes, respectively. The signs of the computed coupling constants are not consistent with the observed magnetic properties, but do conform to what is expected in ethynylbenzene-bridged systems,[108,68] namely, ferromagnetic coupling for meta-bridged **4** and antiferromagnetic coupling for para-bridged **5**. We note that the magnitudes of the calculated coupling constants for models of **4** and **5** are much smaller than those computed for similar transition-metal based systems.[68] As with the model mononuclear complex calculation, net spin density (ρ_α-ρ_β) plots generated for models of **4** and **5** (Figure 8) show very little bridging-ligand density, no matter what spin states are used for the U(IV) constituent ions. We conclude that ethynylbenzene ligands such as DEB and TEB are generally competent for mediating J-coupling in transition metal complexes, but not for U(IV) with the NN′$_3$ ancillary ligand set in the tbp coordination geometry.

Summary and Outlook

We have prepared a structurally related family of penta- and hexacoordinate U(IV) complexes bridged by anionic ethynylbenzene ligands, and have used multiple techniques to characterize them. Despite the fact that all the compounds presented in this study give non-magnetic ground states at low temperature, consistent with those described elsewhere in the literature,[94−98,100−105,109−111] fits to the adjusted magnetic susceptibility data point to weak ferromagnetic communication between the uranium centers in the di- and trinuclear pentacoordinate U(IV)-containing compounds **4**, **5**, and **6**. Theoretical calculations do not reproduce the observed types of coupling, but do show that communication through the ethynylbenzene bridge is weak for these U-containing species, and likely subject to significant perturbation by spin−orbit coupling. In turn, this may inform future work toward utilizing actinide elements in the generation of new SMMs.

The observed and calculated magnetic properties of this family of U(IV)-containing complexes can be rationalized in the following way. First, a trigonal bipyramidal ligand field provides the potential to observe a triplet ground state for a U(IV) ion, but spin−orbit coupling causes admixture of excited singlet states, reducing paramagnetic contributions. Second, although calculations point to π-type orbital overlap between acetylide ligands and the 5f orbitals of the U(IV) ion, negligible spin density from the metal leaks onto the bridging ligands, leading to weak ferromagnetic coupling via application of Hund's rule.

The lack of delocalization for U(IV) is likely due to a metal-bridging ligand energy mismatch. Andersen's bis-diazenylbenzene ligand[59] or a dicyanobenzene species is hypothesized to provide a better energy match. In addition, because the f orbitals that can interact with acetylide π orbitals also have σ interactions with the NN′$_3$ ligand, substituent changes on the tetradentate ligand may also give rise to significant changes in magnetism. Computational studies focusing on meta and para substituted uranium complexes with modified bridging ligands are planned, and the results will be compared with transition-metal based systems, both experimentally and computationally.

We have also shown that the monomeric arylacetylide complex, **3**, undergoes a reversible redox couple assignable to a U(IV/V) process. This offers a route toward half integer actinide-containing spin systems where the DEB ligand may enjoy more substantial orbital overlap with U(III) or U(V) ions. Efforts to find chemically accessible reductions or oxidations of **1**, **4**−**6**, and related compounds to U(III) or U(V) are underway. Precedent for this possibility is given by the recent report of organometallic U(IV) complex oxidation by Cu(I) phenylacetylide.[112]

Acknowledgment. This research was supported by Colorado State University and the ACS Petroleum Research Fund (44691-G3). We thank Ms. Susie Miller and Prof. Oren Anderson for advice on crystal structure refinements, Dr. Christopher Rithner for assistance with NMR data collection, Mr. Don Heyse for assistance with EPR data collection, and Dr. P. Jeffrey Hay and Prof. C. M. Elliott for helpful conversations.

Supporting Information Available: X-ray crystallographic files (cif); full characterizations of complexes **1**−**6**, coordinates for calculated model complexes, and full citation for reference 85 (pdf). This material is available free of charge via the Internet at http://pubs.acs.org.

(108) Ovchinnikov, A. A. *Theor. Chim. Acta* **1978**, *47*, 297–304.
(109) Boudreaux, E. M., L. N. *Theory and Application of Molecular Paramagnetism*; John Wiley & Sons: New York, 1976.
(110) Suski, W.; Baran, A.; Folcik, L.; Wochowski, K.; Mydlarz, T. *J. Alloys Compd.* **1992**, *181*, 249–255.
(111) Karbowiak, M.; Drozdzynski, J. *J. Alloys Compd.* **1998**, *271*, 863–866.
(112) Graves, C. R.; Scott, B. L.; Morris, D. E.; Kiplinger, J. L. *Organometallics* **2008**, *27*, 3335–3337.